Liquid Crystals
Publication details, including instructions for authors and subscription information:
http://www.informaworld.com/smpp/title~content=t713926090

Optical behaviour of photoimageable cholesteric liquid crystal cells with various novel chiral compounds

Jui-Hsiang Liu[a]; Po-Chih Yang[b]
[a] Department of Chemical Engineering and Institute of Electro-optics, National Cheng Kung University, Tainan, Taiwan 70101, ROC [b] Department of Chemical Engineering, National Cheng Kung University, Tainan, Taiwan 70101, ROC

To cite this Article Liu, Jui-Hsiang and Yang, Po-Chih(2005) 'Optical behaviour of photoimageable cholesteric liquid crystal cells with various novel chiral compounds', Liquid Crystals, 32: 5, 539 — 551
To link to this Article: DOI: 10.1080/02678290500117654
URL: http://dx.doi.org/10.1080/02678290500117654

Liquid Crystals, Vol. 32, No. 5, May 2005, 539–551

Optical behaviour of photoimageable cholesteric liquid crystal cells with various novel chiral compounds

JUI-HSIANG LIU*† and PO-CHIH YANG‡

†Department of Chemical Engineering and Institute of Electro-optics, National Cheng Kung University, Tainan, Taiwan 70101, ROC

‡Department of Chemical Engineering, National Cheng Kung University, Tainan, Taiwan 70101, ROC

(*Received 28 September 2004; in final form 7 February 2005; accepted 9 February 2005*)

In theory, both polarity and steric hindrance are basic factors which affect molecular interactions. To investigate the optical properties and steric structures of chiral compounds having different chiral moieties which affect the wavelength of light reflection in liquid crystal (LC) cells, a series of novel chiral compounds and azobenzene derivatives were synthesized. The liquid crystalline phases of the compounds were identified using small angle X-ray diffraction, differential scanning calorimetry and polarizing optical microscopy. Cholesteric LC cells with various synthesized chiral dopants which selectively reflect visible light were first prepared, the photochemical switching behaviour of colours was then investigated, with special reference to the change in transmittance in cholesteric LC cells containing an azobenzene derivative as a photoisomerizable guest molecule. Reversible isomerization of azobenzene molecules occurred in the cholesteric systems, resulting in a depression of T_{ChI} and a shift of the selectively reflected wavelength. We discuss the photochemically driven change in the helical pitch of the cholesteric LCs with respect to structural effects involving the chiral moieties. Molecular interactions caused by the added dopants, reliability and stability of the photoisomerization, and UV irradiation effects on the cholesteric LC cells were also investigated. A real image was recorded through a mask on a cholesteric LC cell fabricated in this investigation.

1. Introduction

Because the optical properties of liquid crystals (LCs) respond to the internal or external environment, much attention has been paid to their application in optical devices. Among these materials, cholesteric LCs have the characteristic optical property of reflecting a circularly polarized component of light, whose wavelength λ corresponds to the product of the pitch P and the average of the refractive index n $\lambda = nP$. When λ is in the visible region, an iridescent reflected colour is seen. The reflected colour (cholesteric pitch) is influenced by the temperature, external force, magnetic field, electric field and chemical composition [1]. Many studies have been carried out on the pitch change due to the modification of chemical compositions in mixed cholesteric LC systems [1–5]. Among these, the change in the helical pitch caused by photochemical reactions in cholesteric LCs is of special interest [3–5]. The cholesteric pitch changes because photochemical reactions alter the composition of the cholesteric LCs.

Photochemical control of the phase structures of LCs has been widely studied in the field of optical devices such as optical switching [6–10]. It is well known that azobenzene undergoes isomerization from *trans* to *cis* under ultraviolet light irradiation, while the *cis*-form can return to the *trans*-form either photochemically or thermally. Such a geometrical change can produce concomitant changes in physical and chemical properties of the azobenzene and in the microenvironments around it. Such photonic control has been mainly applied in the nematic phase by means of transmission, reflection, and light-scattering systems [11–14]. When azobenzene is embedded in a nematic LC, the two isomers produce different environments, characterized by the two different molecular shapes. Thus, optical information can be detected as changes in optical properties such as birefringence, before and after photoisomerization of the azobenzene molecules in the LC systems. It has also been shown that *trans–cis* photoisomerization of a guest azobenzene compound with no chiral moiety may cause a change in the cholesteric pitch of a host cholesteric LC [15, 16]. Kurihara *et al.* also studied the photochemical

*Corresponding author. Email: jhliu@mail.ncku.edu.tw

Liquid Crystals
ISSN 0267-8292 print/ISSN 1366-5855 online © 2005 Taylor & Francis Group Ltd
http://www.tandf.co.uk/journals
DOI: 10.1080/02678290500117654

switching of a compensated nematic LC; this was prepared by adding a chiral azobenzene compound and a non-photochromic chiral compound with opposite twisting ability to a host LC [17, 18]. Recently, Ruslim and Ichimura reported conformational effects on the photochemical change in helical structure of a cholesteric phase, by the photoisomerization of azobenzene compounds having chiral moieties at different positions [19, 20].

In principle, specific rotation reveals the characteristic of net vector of the polarity of the chiral molecules on plane polarized light. The 'polar effect' should also influence host LC molecules. The results of polar and steric interactions between chiral dopants and host LCs are revealed as the helical twisting power (HTP). In this study, a series of mesogenic chiral compounds and non-mesogenic chiral azobenzene derivatives, having different chiral moieties and steric structures, were synthesized. The effect of molecular structures on the selective light reflection of cholesteric LC cells was investigated. Photochemical switching behaviour of colours were studied, with special reference to the change in transmittance, by means of cholesteric LC systems containing an azobenzene derivative as a photoisomerizable guest molecule. From the results of this investigation, it is expected that these cholesteric LC cells may have potential in applications for photoswitchable reflectors, shutters, and photocontrollable and imageable coatings.

2. Experimental

2.1. *Characterization*

FTIR spectra were recorded on a Jasco VALOR III (Tokyo, Japan) FTIR spectrophotometer. Nuclear magnetic resonance (NMR) spectra were obtained on a Bruker AMX-400 (Darmstadt, Germany) high resolution NMR spectrometer. Optical rotations were measured at 30°C in $CHCl_3$ using a Jasco DIP-370 polarimeter with the D-line of sodium ($\lambda = 589$ nm). The measurements were performed using 1% solutions of substances in $CHCl_3$.

Differential scanning calorimetry (DSC) was conducted with a Perkin-Elmer DSC 7 instrument at heating and cooling rates of 5–10 K min^{-1} in a nitrogen atmosphere. Phase transitions were investigated with an Olympus BH-2 polarizing optical microscope equipped with a Mettler hot stage FP-82; the temperature scanning rate was 5–10 K min^{-1}.

UV spectroscopy measurements were carried out with a Jasco V-550 UV-vis spectrophotometer. X-ray diffraction (XRD) data were recorded on a Rigaku RINT 2500 series with Ni-filtered CuK_α radiation. The sample in a quartz capillary was held in a temperature-controlled cell (Rigaku LC high temperature controller). The transmittance spectra were recorded with a USB-2000 fibre optic spectrometer from Oceanoptics Company. UV light (365 nm) with an intensity of 0.4 mW was used as a pumping light to induce isomerization of azo-molecules in the cholesteric LC systems.

2.2. *Materials and synthesis*

ZLI-2293, a commercially available eutectic mixture of several low molecular mass nematic LCs, was purchased from Merck (Darmstadt, Germany) and was used as a host LC without further purification. This LC shows a nematic phase over a wide range of temperature to 85°C. The chiral and azobenzene compounds used in this investigation are listed in scheme 1, and synthetic methods are as shown in schemes 2, 3 and 4 [21–24]. The products were identified by spectrophotometry.

Chiral agent S811 (Merck, Germany), which induces a left-handed helical optical rotation, was dissolved in the host nematic LC to produce a cholesteric LC phase. Chiral compounds **3**, **5** and **6**, with different mesogenic cores and chiral moieties, were synthesized. Chiral dopants **7** (cholesteryl oleate) and **8** (cholesteryl pelargonate) were purchased from Acros (Geel, Belgium) and used without further purification. The cholesteric to isotropic phase transition temperature of chiral dopant **7** is 42.0°C. Chiral dopant **8** showed a cholesteric phase from 80.5 to 92.0°C during heaing. We also synthesized AzoA and AzoB azobenzene derivatives containing chiral (-)-amyl and (-)-bornyl groups, respectively.

2.2.1. (S)-(-)-2-Methylbutyl 4-hydroxybenzoate (1). A mixture of (*S*)-2-methyl-1-butanol (13.2 g, 150 mmol) and 4-hydroxybenzoic acid (13.8 g, 100 mmol) in dry benzene (150 ml), with a few drops of sulphuric acid, was heated under reflux with a Dean Stark trap for 24 h. The reaction mixture was washed with 5% aqueous $NaHCO_3$ and water, dried over $MgSO_4$, and evaporated. The product was purified by column chromatography (silica gel, ethyl acetate/hexane = 1/4) to afford a light yellow oil; yield 14.7 g (70.6%). FTIR (cm^{-1}): 3320 (OH), 2961, 2865 (CH_2), 1692 (C=O in Ar–COO–), 1612, 1510 (C–C in Ar). ^1H NMR ($CDCl_3$, δ = ppm): 0.87–1.07 (m, 6H, CH_3), 1.24–1.61 (m, 2H, CH_2), 1.80–1.92 (m, 1H, CH), 4.15 (t, 2H, $COOCH_2$), 6.92–7.95 (m, 4H, aromatic).

2.2.2. 4-Decyloxybenzoic acid (2). 4-Hydroxybenzoic acid (16.5 g, 120 mmol) was dissolved in EtOH (42 ml) and H_2O (18 ml). KOH (17.8 g, 317.8 mmol) and a

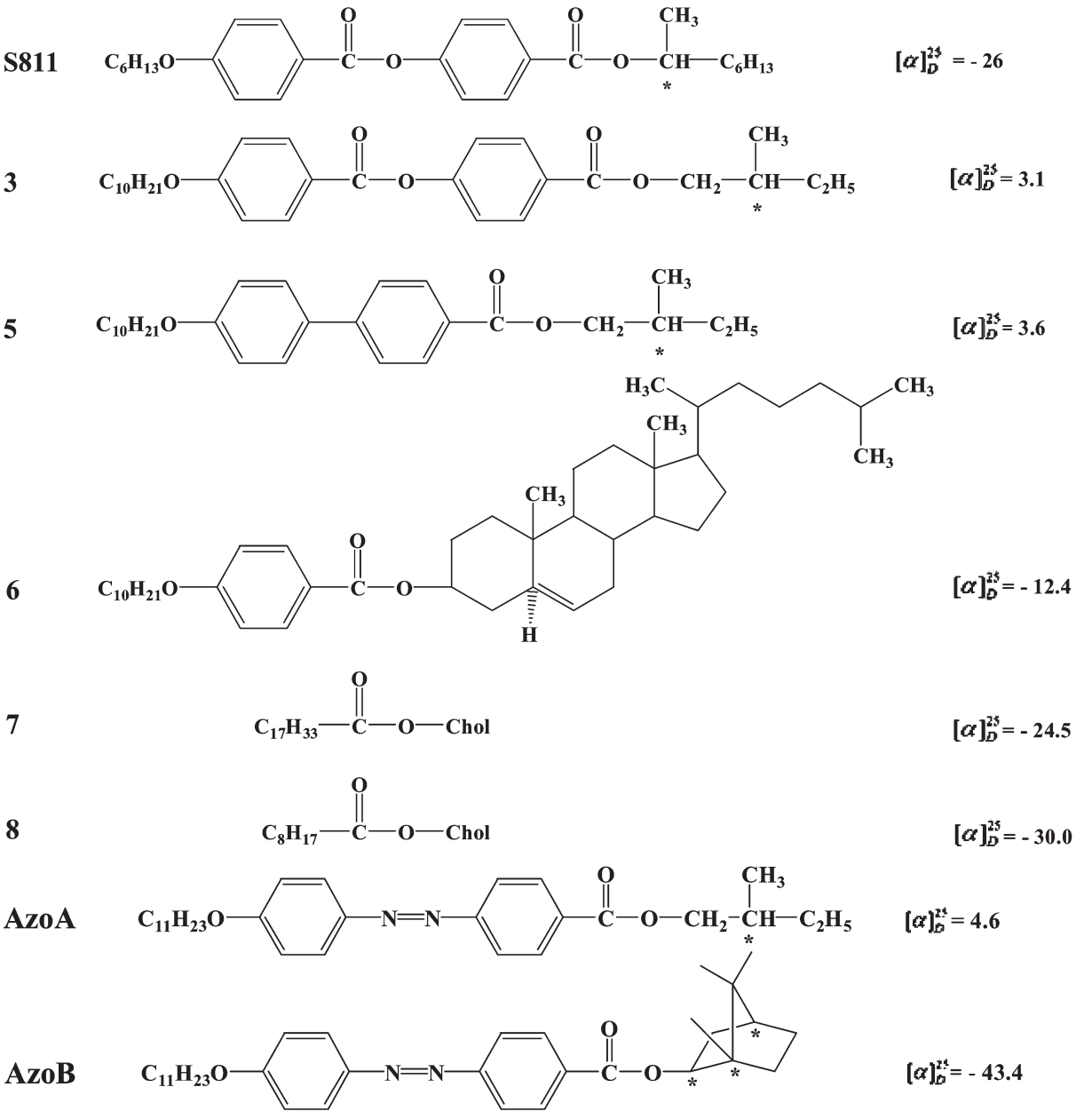

Scheme 1. Chiral and azobenzene compounds used in this study.

catalytic amount of KI dissolved in EtOH (50 ml) were added dropwise to the solution. 1-Bromodecane (31.8 g, 144 mmol) was then added, and the solution heated at reflux for 24 h. The resulting mixture was poured into water and extracted with diethyl ether. The aqueous phase was acidified with dilute HCl and the resulting precipitate filtered off and washed several times with water. The crude product was recrystallized twice from EtOH/H_2O (4/1); yield 20.5 g (61.5%), T_m 85°C. FTIR (cm^{-1}): 3250 (OH), 2935, 2856 (CH_2), 1692 (C=O in Ar–COO–), 1600, 1524 (C–C in Ar). ^1H NMR (DMSO, δ=ppm): 10.05 (s, 1H, COOH), 0.92–1.15 (m, 3H, CH_3), 1.23–1.56 (m, 16H, CH_2), 4.1 (t, 2H, OCH_2), 7.08–8.12 (d, 4H, aromatic).

2.2.3. (S)-(+)-2-Methylbutyl 4-decyloxybenzoyloxybenzoate (3). Compound **1** (2.08 g, 10 mmol) and compound **2** (2.78 g, 10 mmol) were dissolved in CH_2Cl_2 (50 ml) at room temperature. *N*,*N*′-dicyclohexylcarbodiimide (DCC) (3.1 g, 15 mmol) and *N*,*N*-dimethylaminopyridine (DMAP) (0.12 g, 1 mmol)were dissolved in CH_2Cl_2 (40 ml), and the two

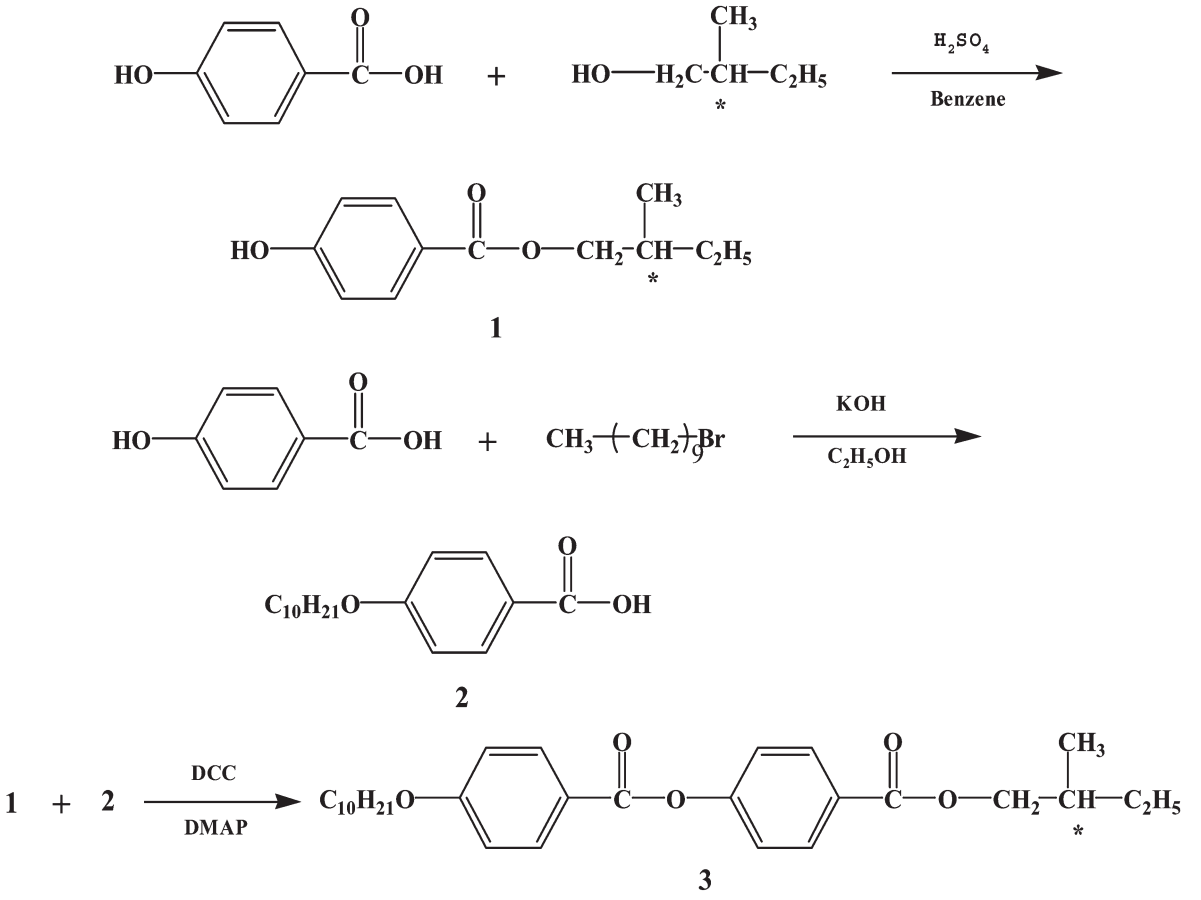

Scheme 2. Synthesis of chiral compound **3**.

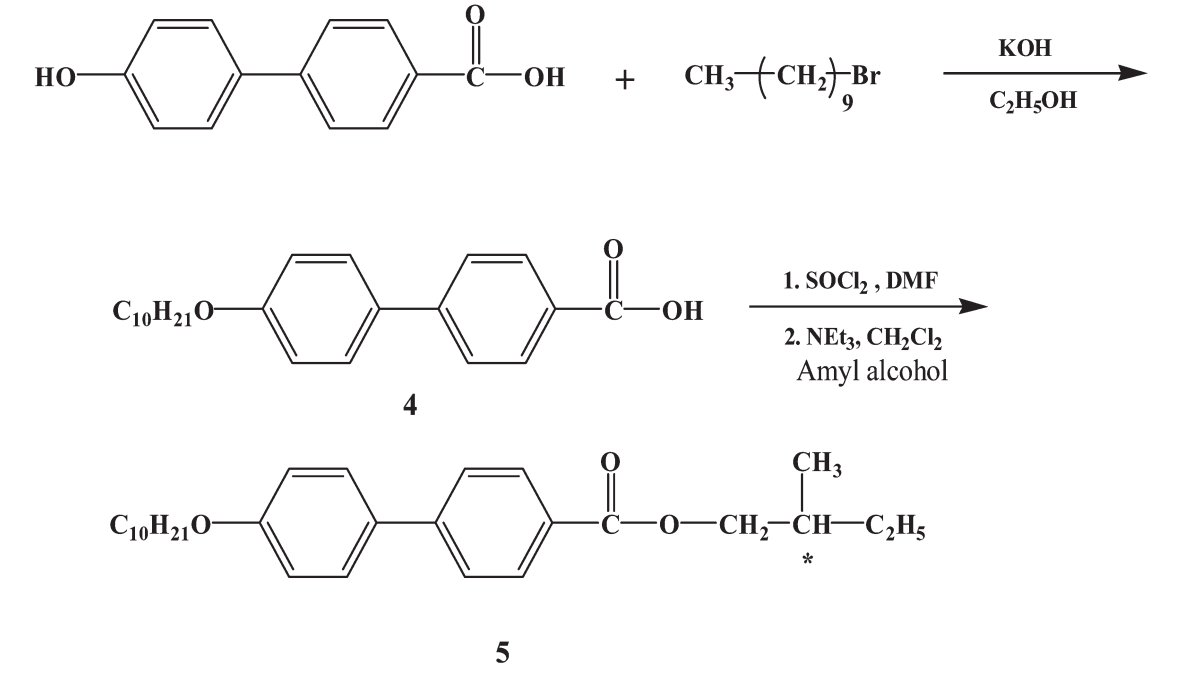

Scheme 3. Synthesis of chiral compound **5**.

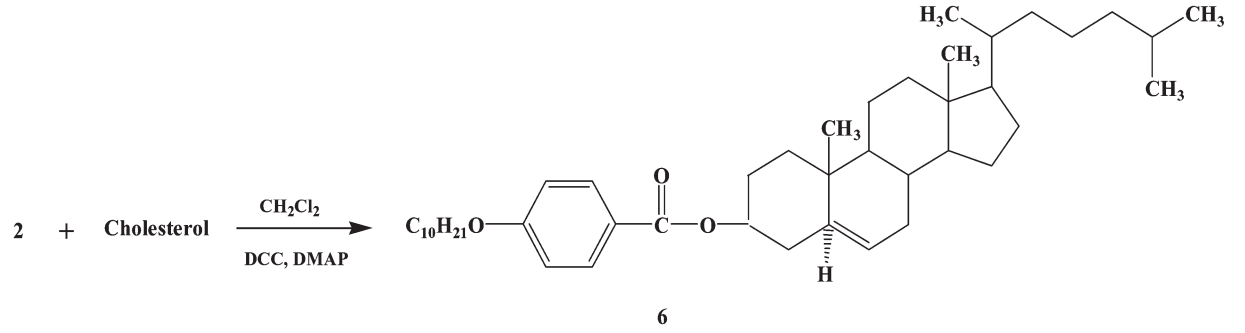

6

Scheme 4. Synthesis of chiral compound **6**.

solutions mixed and stirred for 1 day at r.t.. The resulting solution was washed with water, dried over $MgSO_4$, and evaporated. The crude product was purified by column chromatography (silica gel, ethyl acetate/hexane=1/6) and recrystallized twice from EtOH; yield 2.93 g (62.6%). FTIR (cm^{-1}): 2925, 2851 (CH_2), 1720 (C=O in Ar–COO–), 1602, 1498 (C–C in Ar). ^1H NMR ($CDCl_3$, δ=ppm): 0.84–1.06 (m, 9H, CH_3), 1.19–1.56 (m, 18H, CH_2), 1.82–1.90 (m, 1H, CH), 4.05–4.10 (m, 4H, OCH_2), 7.15–8.14 (d, 8H, aromatic). From the UV-Vis spectrum, λ_{max}=272 nm ($CHCl_3$). Elemental analysis for $C_{29}H_{40}O_5$(468): calcd, C 74.36, H 8.55; found, C 74.37, H 8.63%.

2.2.4. 4-(4-Decyloxyphenyl)benzoic acid (4). 4-(4-Hydroxyphenyl)benzoic acid (10.0 g, 46.7 mmol) was dissolved in EtOH (200 ml) and H_2O (30 ml). KOH (7.8 g, 140 mmol) and a catalytic amount of KI dissolved in EtOH (60 ml) was added dropwise to the solution. 1-Bromodecane (11.3 g, 51 mmol) was then added, and the solution heated at reflux for 24 h. The resulting mixture was poured into water, and the aqueous phase acidified with dillute HCl. The resulting precipitate was filtered off, washed several times with water and recrystallized from glacial acetic acid/ethanol (2/3); Yield 9.72 g (58.6%), T_m 160°C. FTIR (cm^{-1}): 3265 (OH), 2927, 2855 (CH_2), 1712 (C=O in Ar–COO–), 1606, 1505 (C–C in Ar). ^1H NMR ($CDCl_3$, δ=ppm): 9.95 (s, 1H, COOH), 0.86–1.12 (m, 3H, CH_3), 1.16–1.48 (m, 16H, CH_2), 4.06–4.12 (t, 2H, OCH_2), 6.88–7.76 (d, 8H, aromatic).

2.2.5. (S)-(+)-2-Methylbutyl 4-(4-decyloxyphenyl)-benzoate (5). Thionyl chloride (4.76 g, 40 mmol) was added dropwise to a mixture of compound **4** (1.77 g, 5 mmol) and 5 drops of dimethylformamide in dry CH_2Cl_2 (40 ml); the mixture heated under reflux for 3 h. Excess thionyl chlodide was then removed under reduced pressure. 4-(4-Decyloxyphenyl)benzoyl chloride was obtained as a yellow solid; it was dissolved in dry CH_2Cl_2 (40 ml), and added slowly to a solution of (*S*)-2-methyl-1-butanol (0.44 g, 5 mmol) and trimethylamine (0.61 g, 6 mmol) in dry CH_2Cl_2 (30 ml). The mixture was stirred at r.t. for 24 h, then washed with water, dried over $MgSO_4$, and evaporated. The crude product was purified by column chromatography (silica gel, ethyl acetate/hexane=1/6) and recrystallized twice from EtOH; yield 1.19 g (56.4%). FTIR (cm^{-1}): 2918, 2849 (CH_2), 1715 (C=O in Ar–COO–), 1603, 1528 (C–C in Ar). ^1H NMR ($CDCl_3$, δ=ppm): 0.90–1.45 (m, 9H, CH_3), 1.12–1.35 (m, 18H, CH_2), 1.80–1.95 (m, 1H, CH), 4.01–4.15 (m, 4H, OCH_2), 6.88–7.76 (d, 8H, aromatic). UV-Vis: λ_{max}=298 nm ($CHCl_3$). Elemental analysis for $C_{28}H_{40}O_3$(424): calcd, C 79.25, H 9.43; found, C 79.15, H 9.51%.

2.2.6. (-)-Cholesteryl 4-decyloxybenzoate (6). Compound **2** (2.78 g, 10 mmol) and cholesterol (3.86 g, 10 mmol) were dissolved in CH_2Cl_2 (60 ml) at room temperature. DCC (3.1 g, 15 mmol) and DMAP (0.12 g, 1 mmol) were dissolved in CH_2Cl_2 (40 ml) and added to the solution. The reaction mixture was stirred for 1 day at r.t., washed with water, dried over $MgSO_4$ and evaporated. The crude product was purified by column chromatography (silica gel, ethyl acetate/hexane=1/6) and recrystallized twice from EtOH; yield 3.89 g (60.2%). FTIR (cm^{-1}): 2932, 2852 (CH_2), 1699 (C=O in Ar–COO–), 1605, 1501 (C–C in Ar). ^1H NMR ($CDCl_3$, δ=ppm): 0.86–1.15 (m, 18H, CH_3), 1.31–2.32 (m, 44H, CH_2), 4.01 (d, 2H, OCH_2), 4.83 (s, 1H, Ar–COOCH), 5.4 (s, 1H, C=CH), 7.12–7.97 (d, 4H, aromatic). UV-Vis: λ_{max}=258 nm (in $CHCl_3$). Elemental analysis for $C_{44}H_{70}O_3$(646): cald, C 81.73, H 10.84; found, C 81.54, H 10.82%.

2.2.7. (+)-Amyl 4-(4-undecyloxyphenylazo)benzoate (AzoA). Compound AzoA (and AzoB) was synthesized by procedures similar to those described in the literature [25]; yieid 53%. Elemental analysis for

$C_{29}H_{42}N_2O_3$(466): cald, C 74.68, H 9.01, N 6.01; found, C 74.57, H 9.13, N 6.05%.

2.2.8. (-)-Bornyl 4-(4-undecyloxyphenylazo)benzoate (AzoB). Yieid 42%. Elemental analysis for $C_{34}H_{48}N_2O_3$ (532): cald, C 76.69, H 9.02, N 5.26; found, C 76.78, H 9.11, N 5.21%.

2.3. *Fabrication of liquid crystal cells*

ITO plates were cleaned with detergent solution, then ultrasonically washed with water followed by acetone, for 20 and 60 min, respectively. The ITO plates were dried in vacuum; one side was coated with polyvinyl alcohol (M_w=20 000), dried and then rubbed to provide homogeneous alignment. Glass cells, each with a pair of parallel pre-rubbed ITO plates and a 12 μm gap, were fabricated. After filling with LC mixture, each cell was sealed with epoxy resin. The optical properties of the LC cells were investigated. Detailed compositions of the sample cells are summarized in table 2.

Table 1. Phase transition temperature (°C) and optical rotation (°) of the chiral compounds. Cr=crystal, SmA=smectic A, N*=chiral nematic, I=isotropic.

Sample	Heating cycle	Cooling cycle	$[\alpha]_D^{25}$[a]
3	Cr 50.6 SmA 57.5 I	I 53.8 SmA 33.6 Cr	3.1
5	Cr 47.0 SmA 61.9 I	I 58.8 SmA 26.7 Cr	3.6
6	Cr 107.1 SmA 167.3 N* 203.7 I	I 203.1 N* 141.9 SmA 64.7 Cr	−12.4
7	Cr 44.5 I	I 42 Cr	−24.5
8	Cr 80.5 SmA 92 I	I 77.5 Cr	−30
Azo A	Cr 85.5 I	I 71.6 Cr	4.6
Azo B	Cr 105.4 I	I 87.1 Cr	−43.4

[a]Specific rotation of compounds, 0.1g in 10 ml $CHCl_3$.

3. Result and discussion

The thermal properties and the phases of the synthesized compounds are summarized in table 1; they are all chiral derivatives. Phase transition temperatures and specific rotations of the compounds were estimated by DSC and polarimetry, respectively. Liquid crystal phases appeared at different points during the heating and cooling cycles. Depending on the molecular structures, chirality and the ligands around the chiral centre, optical right and left rotations of the compounds were observed. Generally, the high π-electron density benzene ring in a molecule is an important factor in the formation of LC phases; as shown in scheme 1, the LC molecules **3**, **5** and **6** all contain at least one benzene ring. The commercially available compounds **7** and **8** also exhibit LC phases, although they have only the cholesteryl group and no benzene ring. Cholesteric LC phases usually appear in most cholesterol derivatives.

Liquid crystal textures were confirmed using DSC, XRD and polarizing optical microscopy (POM). Figures show the textures of compounds **3**, **5** and **6** at various temperatures. The LC phases were confirmed by comparing the textures with literature reports, and identified using small angle XRD. The *d*-spacing estimated from the peak in the small angle data for chiral compounds **3** and **5** was 22.12 and 22.17 Å, respectively, suggesting that the phases of compounds **3** and **5** were smectic A (SmA). As shown in scheme 1, compound **6** contains a cholesteryl group having multiple chiral centres; the estimated *d*-spacing for

Table 2. Effect of chiral dopants on reflection wavelength of cholesteric cells.

Sample cell	Chiral dopant	Weight ratio	λ_0/nm[b] Before	λ_0/nm[b] After	T_{ChI}(°C)[c]
1	—	10:3:0	695	—	72
2	—	10:4:0	596	—	66
3	3	10:3:0.5	718	—	68
4	5	10:3:0.5	744	—	69
5	6	10:3:0.5	678	—	74
6	7	10:3:0.5	623	—	66
7	8	10:3:0.5	607	—	68
8	AzoA	10:4:0.1	570	556	64
9	AzoB	10:4:0.1	567	545	65
10	AzoA	10:4:0.3	582	557	63
11	AzoB	10:4:0.3	604	574	63
12	AzoA	10:4:0.5	588	546	60
13	AzoB	10:4:0.5	654	581	61

[a]Weight ratio ZLI-2293: S811: chiral dopant.
[b]Major reflected wavelength, before and after UV irradiation.
[c]T_{ChI}: clearing temperature from cholesteric to isotropic phase.

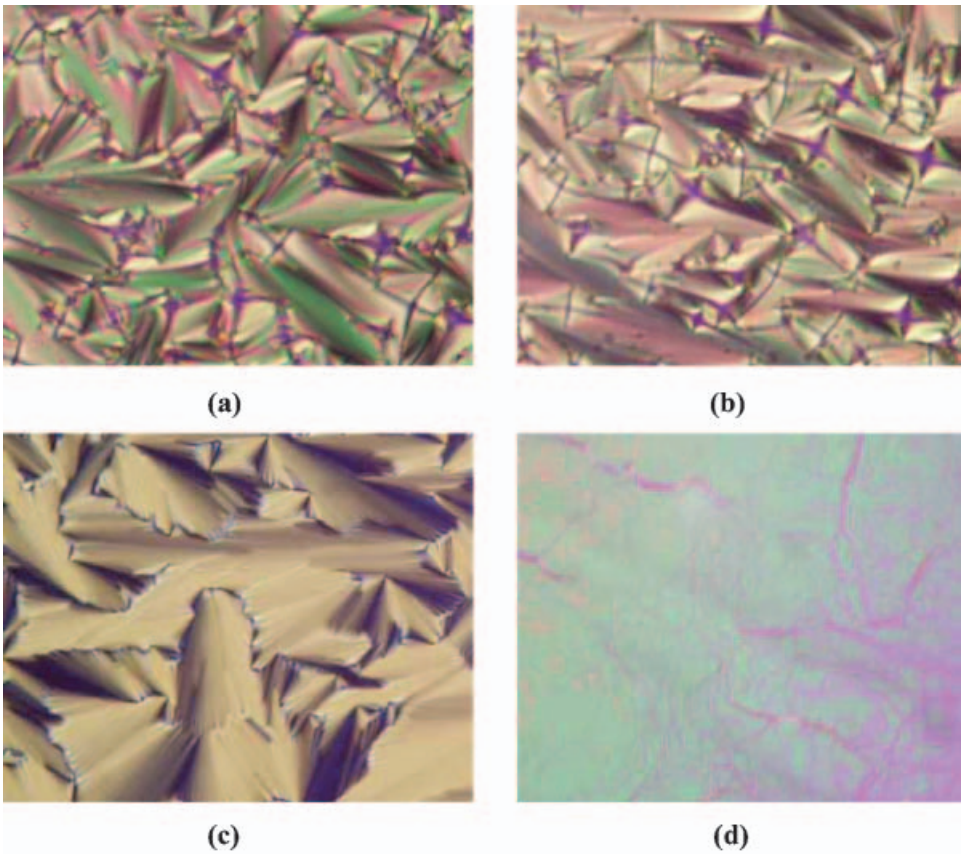

Figure 1. POM textures of (*a*) compound **3** at 41.5°C during cooling, (*b*) compound **5** at 54.5°C during heating, (*c*) compound **6** at 142.5°C and (*d*) at 190.5°C during heating.

compound **6** was 22.11 Å. Compounds **7** and **8** contain the same cholesteryl moiety. As shown in scheme 1, all the derivatives have negative optical rotation. Figures 1 (*c*) and 1 (*d*) show the variation in texture of compound **6** at different temperatures in the heating cycle. These results conform with the data listed in table 1.

Figure 2 shows the UV spectra of compounds AzoA and AzoB in chloroform before and after UV irradiation. Azo derivatives in the *trans*-form show a strong band in the UV region (~360 nm) which is attributed to the π–π* transition, and a weak band in the visible region (~450 nm) due to the n–π* transition. The *trans*-form is generally more stable than the *cis*-form, but each isomer can be converted into the other by light irradiation of the appropriate wavelength. However, the *cis*–*trans* isomerization is thermally stimulated on conversion to the *cis*-isomer. As shown in figure 2, the π–π* band shifts to shorter wavelengths, and the intensity of the n–π* absorption increases. The results of figure 2 show that *trans*-Azo derivatives could be changed to the *cis*-form in 70 s through UV irradiation. AzoA and AzoB were found to have 12 h thermostability. After UV irradiation, although kept in the dark, the Azo derivatives gradually returned to *trans*-isomers.

To investigate the steric and dopant concentration effects on the optical behaviour of cholesteric LC cells, a cholesteric phase was induced by mixing small amounts of chiral compound S811 in the host nematic LC ZLI-2293. The helical pitch of the cholesteric phase is very sensitive to the chemical structure and concentration of chiral dopant molecules. Therefore, it can be expected that the wavelength of reflected light from the induced cholesteric phase would be easily controlled by varying the concentration of the chiral dopant molecules. The major reflected wavelength λ_0 shifted to a shorter wavelength with increase in the concentration of S811, as shown in table 2. This suggests that a higher chiral dopant concentration may decrease the pitch of the cholesteric LC, leading to the blue shift of the cholesteric cell. In samples 1 and 2 (table 2), the LC to isotropic phase transition temperature was depressed. This may be due to the increase of steric hindrance from the added chiral dopant. No wavelength shift with UV irradiation was seen in samples 1–7; a shift did occur,

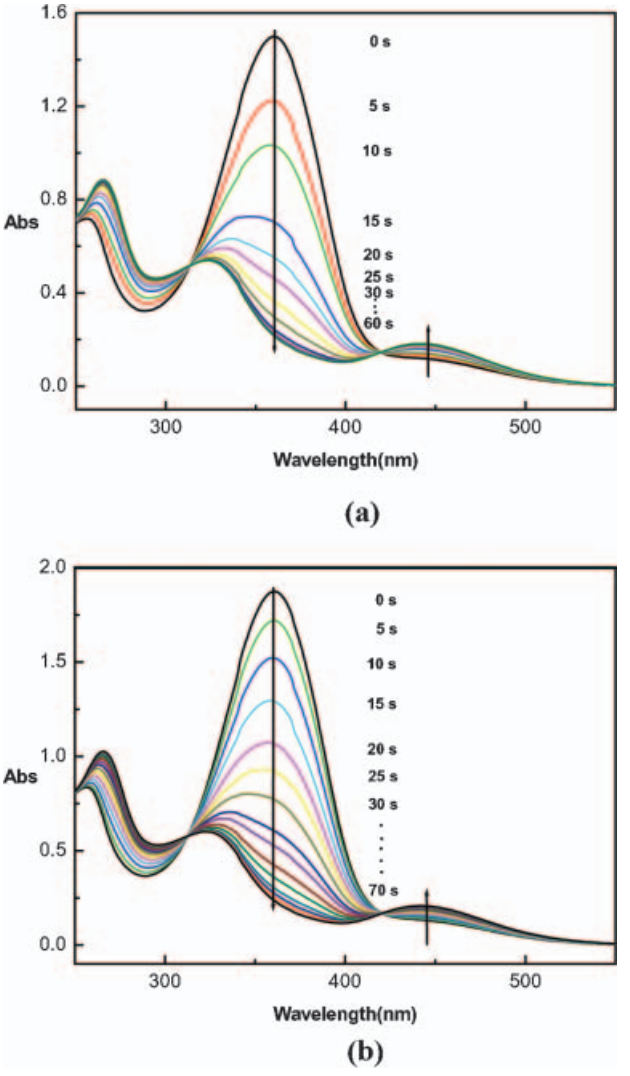

Figure 2. UV spectra of compounds (*a*) AzoA, and (*b*) AzoB in chloroform, before and after UV irradiation.

however, when azo-compounds were used as the chiral dopant. Dopants in the first 7 samples have no photoisomerizable groups.

Figure 3 shows the dependence of the UV-vis spectra of LC cell 2 (ZLI-2293/S811 = 10/4 w/w) on temperature. The reflected light was shifted to a shorter wavelength region and the bandwidth of the reflected light peak was narrowed with increase in temperature. The results suggest that the orientation of the LC molecules was affected by the rise in temperature. A further increase in temperature led to a decrease in intensity of the reflected light, indicating that thermal transition from the cholesteric to the isotropic phase had commenced. Finally, the coloured reflected light vanished completely at the clearing point (T_{ChI}) 66°C, and the cell became transparent. The phase change and molecular orientation of the LCs could also be confirmed by POM.

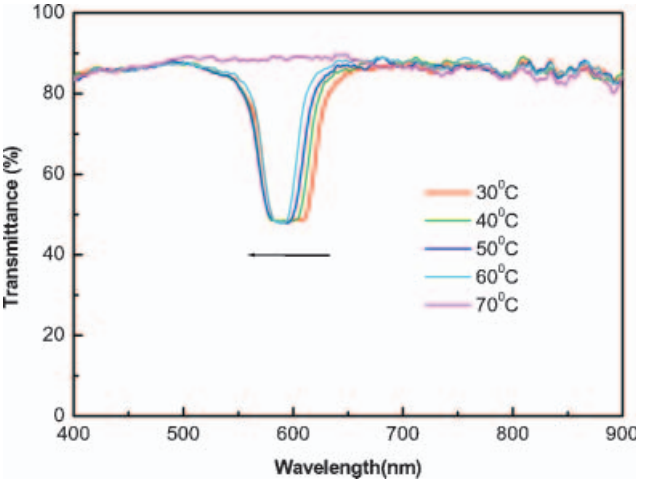

Figure 3. Dependence of UV-vis spectra of sample cell 2 on temperature.

Figure 4 shows POM textures of the same cholesteric LC cell 2 at different temperatures. The different coloured patterns indicate the dependency of cholesteric LC POM textures on temperature.

Right or left *specific rotation* reveals the polar effect of chiral dopants on plane polarized light. The polarity should also operate on liquid crystals. *Helical twisting power* reveals the net polar effect existing in cholesteric LCs. Depending on the molecular interactions, in some cases polar factors from both specific rotation and helical twisting power may operate in the same direction, and show larger effects on the LC molecules. In some cases, the two factors may be in opposition and cancel each other out. However, from the theory of enantiomers, it is clear that enantiomeric chiral dopants should show opposite effects on the same host LC molecules. For a pair of enantiomers, the *R*-form and *S*-form enantiomeric isomers usually exhibit opposite effects. As described in the literature, opposing effects of S811 and R811 on cholesteric pitch have been observed [5]; S811 and R811 are mirror image enantiomers.

To investigate the effect of chiral dopant on the cholesteric LC cells, chiral compounds of scheme 1 were added to the host cholesteric LC. The reflected light wavelength and thermostability of the cells are summarized in table 2. Commercially available S811 with a left-hand optical rotation was dissolved in the host nematic LC ZLI-2293 to produce the cholesteric LC phase used in this investigation. As shown in table 2, samples 1 and 2, a higher concentration of left-rotational S811 causes a blue shift in the cells. In samples 3 to 7, the addition of dopants **3** and **5** causes a red shift; the addition of dopants **6**, **7** and **8** causes a blue shift. This suggests that right-rotational dopants

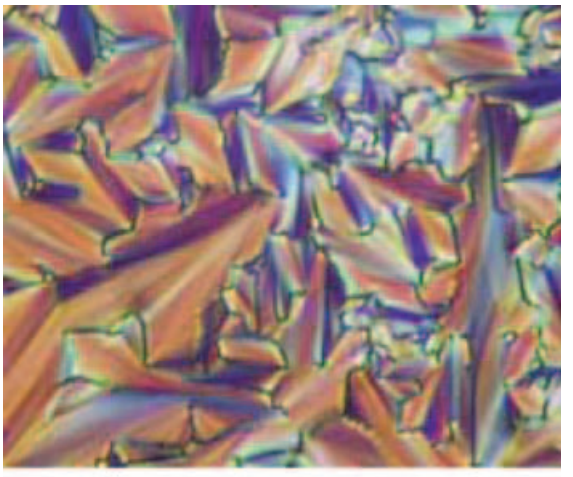

(a)

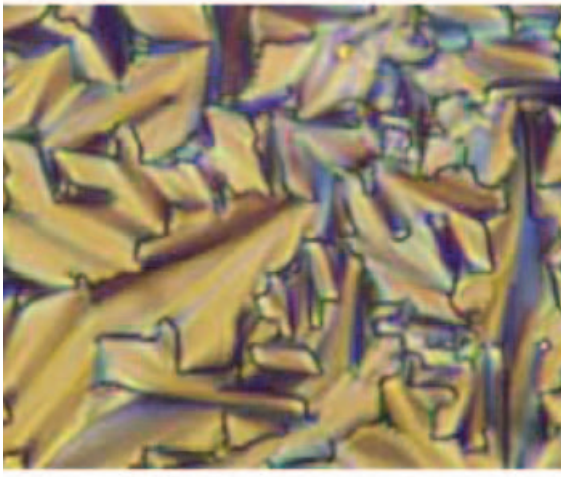

(b)

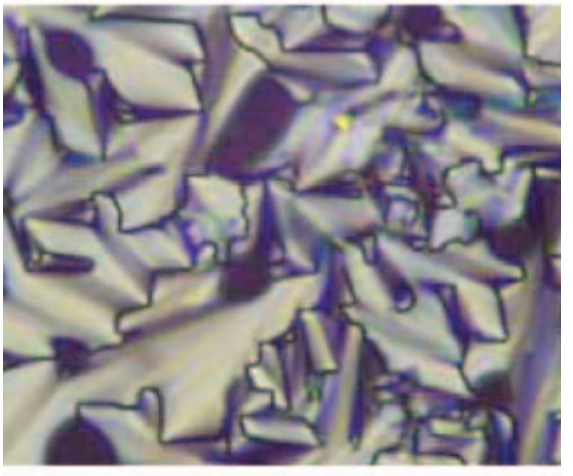

(c)

Figure 4. POM textures of sample cell 2 at (*a*) 30°C, (*b*) 45°C and (*c*) 60°C.

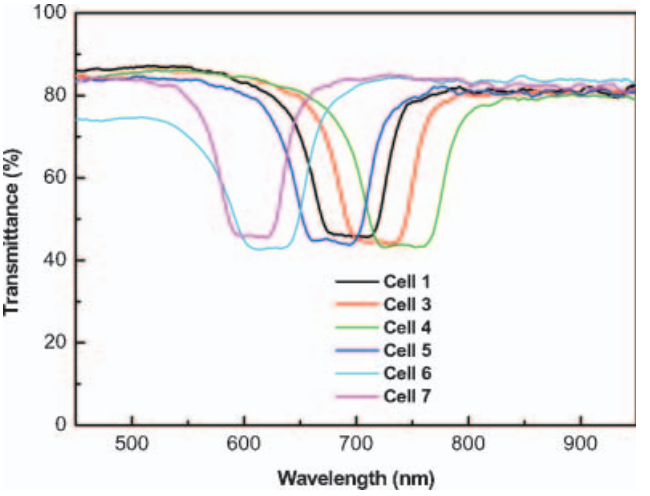

Figure 5. Effect of chiral dopants on reflected light wavelength.

used in this investigation may cancel out the left-twisting effect of the host cholesteric LC. On the other hand, left-rotational dopants may increase the twisting ability of the host cholesteric LC, leading to the blue shift. These results are quite similar to those previously reported [5]. It has also been reported that dopant chirality is a factor which affects the HTP of host LCs [26–30].

The effects of chiral dopants on the UV-vis spectra of the cells is illustrated in figure 5, where variations in the reflected light wavelength due to the addition of the chiral dopants are shown. Temperature effects on the cholesteric LC cells 4 and 5 are summarized in figures 6 (*a*) and 6 (*b*). The cell became transparent when heated to higher than 74°C, consistent with sample 1 behaviour see table 2. Added dopants seem slightly to affect the orientation and thermostability of the host cholesteric LCs leading to a small deviation in both figures.

As shown in scheme 1, AzoA and AzoB consist of different chiral moieties, which exhibit different specific rotations and molecular polarities. As described above, the specific rotation reveals the polar effect of chiral dopants on plane polarized light. In principle, the polar factor should also operate on the host LC molecules. The helical twisting power reveals the net polar effect of chiral dopants on the host LC molecules.

It has already been reported that enantiomeric chiral dopants have opposite effects on the cholesteric pitch [26]. The results suggest that the optical rotation of chiral dopants has some relationship with the cholesteric pitch. As in the case of *R*/*S* and (+)/(−), *R*/*S* indicates the three-dimensional structure of the molecules, and (+)/(−) indicates the polar effect of the molecules on plane polarized light. In principle, they are

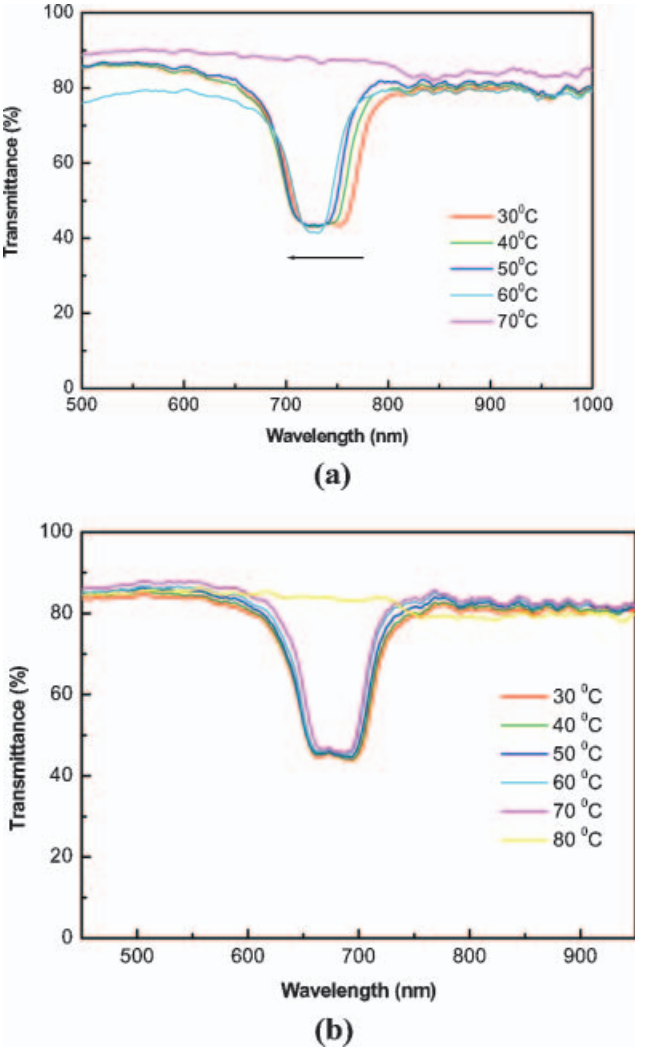

Figure 6. Dependence of UV-vis spectra on temperature with various dopants of (*a*) sample cell 4, and (*b*) sample cell 5.

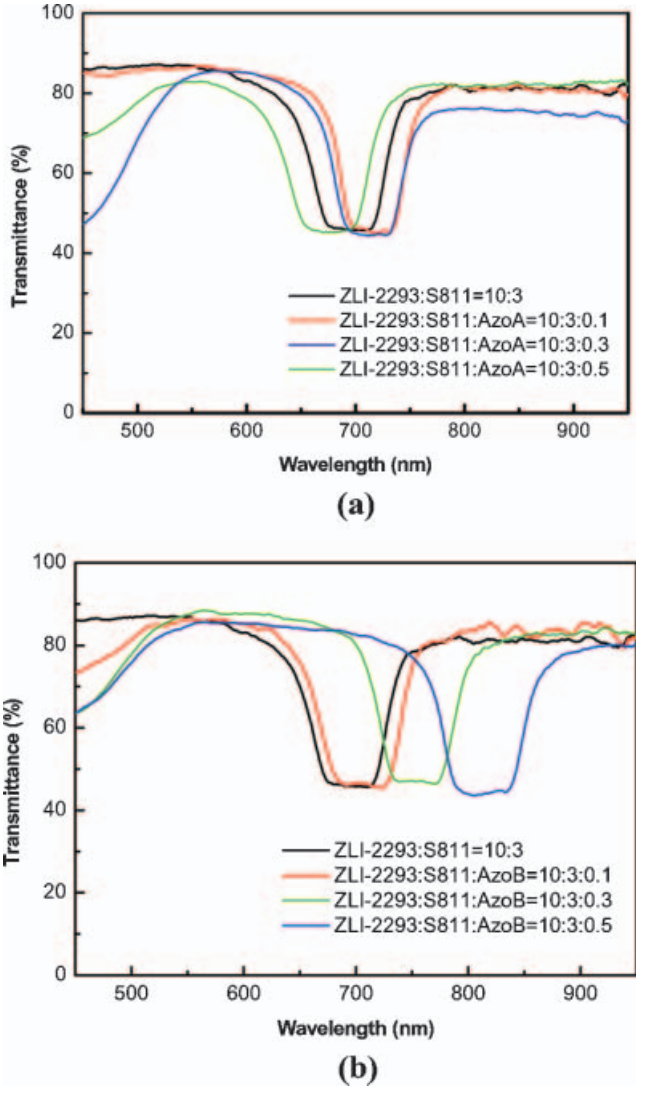

Figure 7. Effect of doping quantity of (*a*) AzoA, and (*b*) AzoB on reflected wavelength.

independent; however, for certain compounds, there are some special relationships between *R*/*S* and (+)/(−). For example, for enantiomers, if the *R*-form shows (+)-rotation, then the *S*-form should show (−)-rotation. If the *R*-form shows (−)-rotation, then the *S*-form should show (+)-rotation.

Considering the (+)/(−) rotation, the addition of AzoA to the cholesteric LC with S811 may cancel out some of the twisting power induced by polar interaction, leading to a red shift. As shown in figure 7 (*a*), further addition of AzoA may cause a stronger molecular interaction between AzoA and the host LC molecules. The orientation and intermolecular forces of the cholesteric LC molecules may be affected by the additional polar factors of the dopants, leading to the final blue shift as shown in figure 7 (*a*).

The intermolecular forces which appear in figure 7 (*b*) appear stronger than those in figure 7 (*a*). Red shifts were obtained, although the AzoB was a left-hand optical rotational compound. The results suggest that the optical rotation should have some polar interaction on the twisting power of the cholesteric LCs. Besides (+)/(−) of the dopants, the direction of the polarity vector of the chiral dopants applied to the LC molecules should also be considered. In this study, the left-rotational dopant favoured the red shift, while, the right-rotational dopant favoured the blue shift.

The intermolecular forces caused by the azo-derivatives can also be seen in figures 8 (*a*) and 8 (*b*). When the cholesteric LC cells with AzoA and AzoB were heated to near the clearing points (T_{ChI}), 55 and 60°C for AzoA and AzoB, respectively, unstable intermediate orientation and

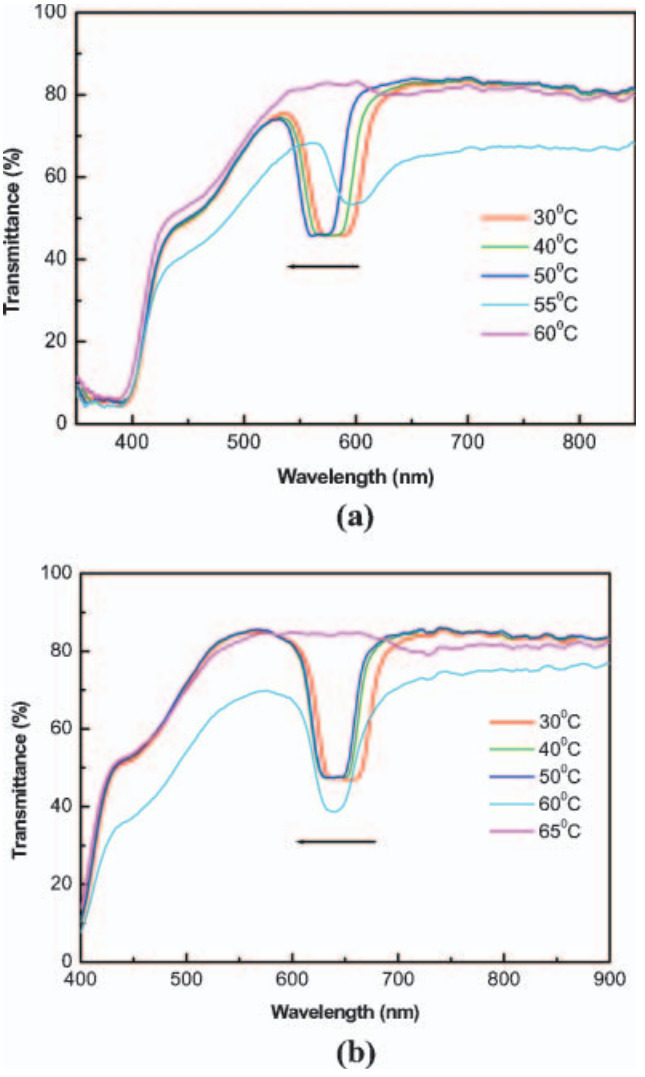

Figure 8. Thermal effects on the cholesteric liquid crystal cells (*a*) 12, and (*b*) 13.

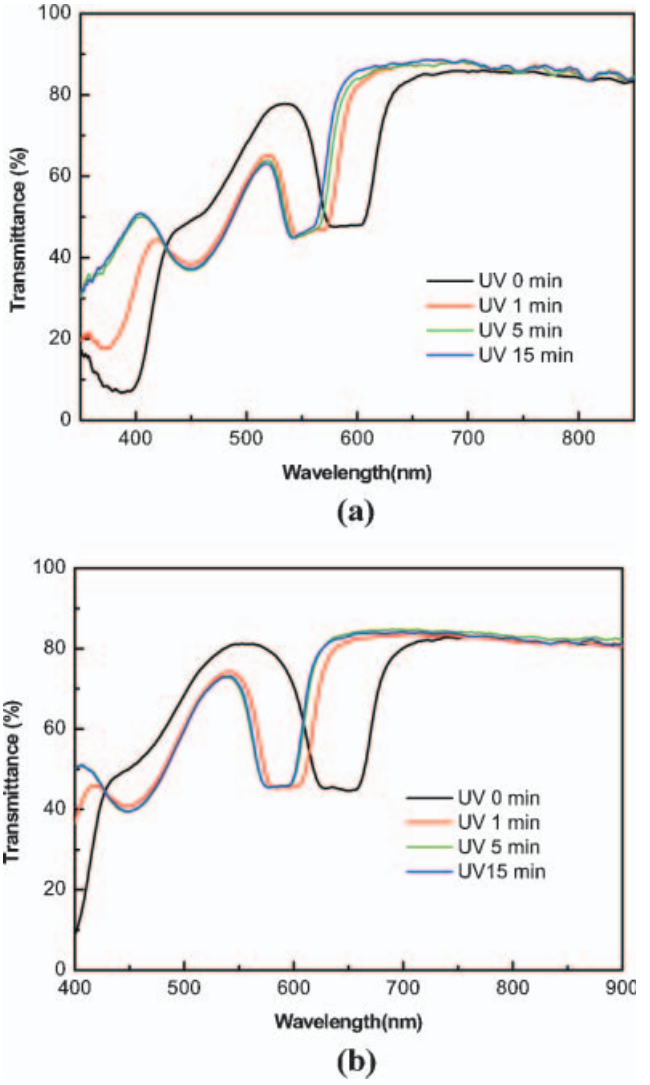

Figure 9. Effect of UV irradiation at room temperature on cholesteric cells (*a*) 12, and (*b*) 13.

absorption were obtained. The baseline of both curves is somewhat worse than for the other cells. Azo-derivatives are thermally unstable compounds; in addition, heating usually increases the mobility of liquid crystals. It appears that the increase in mobility of the azo-derivatives and LCs caused by heating may disturb the orientation of the cholesteric LCs leading to the appearance of the intermediate absorption. Unstable phenomena are usually observed around inter-phase critical points.

Azo-derivatives usually exist in a stable *trans*-configuration. A *trans*-azobenzene molecule may be dissolved in a host LC with no extreme perturbation effect on the molecular orientation of the host LC, because the rod-like shape of the *trans*-azobenzene molecule is similar to that of the host LC molecules. A *cis*-azobenzene molecule, with a bent shape, disorganizes the molecular orientation of the host LC. To investigate the effect of *trans-cis* photoisomerization of azobenzene derivatives having different chiral moieties, and the dependence of the reflected wavelength of cholesteric LCs on UV irradiation, a series of ZLI-2293/S811/Azo composite cells were fabricated and irradiated with UV light. Figures 9 (*a*) and 9 (*b*) show the film transmittance before and after UV irradiation at room temperature for the host cells with AzoA and AzoB dopants, respectively. Blue shifts were observed, as shown in the figures, which may be due to the photoisomerization of the azobenzene derivatives from the *trans*- to *cis*-configuration. When the cells were kept in the dark at room temperature, the photoinduced states returned gradually to their initial states with the initial λ_0 in about 2 hours. This slow recovery was due

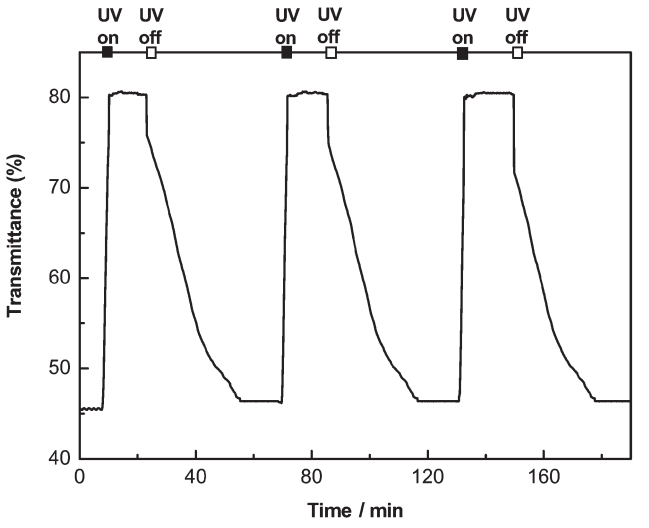

Figure 10. Reliability and stability of cholesteric liquid crystal sample cell 13 at room temperature, observed at 633 nm.

to the slow rate of the thermal *cis* to *trans* back-isomerization of the azobenzene [31]. When the cells were irradiated with UV, the photoinduced states returned quickly to their initial states, bringing about *cis* to *trans* isomerization of the azobenzene derivatives.

Figure 10 shows the reliability and stability of the cholesteric LC cell 13 with AzoB dopant. As shown in figure 9, the transmittance of the cell was detected at 633 nm. As can be seen in figure 10, repeatable and stable ON/OFF optical behaviour was obtained.

To investigate the orientation of LC molecules disturbed by the azo-configuration, the cell containing the host cholesteric LC with AzoA was irradiated with UV at 56°C; the results are summarized in figures 11 (*a–c*). Generally, cholesteric LCs consist of an ordered assembly of molecules, in which nematic LCs are arranged in layers providing an anisotropic environment. Therefore, the *trans*-azobenzene molecule with its rod-like shape is beneficial for the stabilization of the cholesteric phase. On the other hand, the bent *cis*-azobenzene molecule tends to disorganize the orientational order, resulting in a lowering of T_{ChI}, since it acts as an impurity in the system. Hence the shift of the reflected wavelength induced by UV irradiation at 365 nm is closely related to a lowering of T_{ChI} caused by an accumulation of the *cis*-azobenzene molecule, which implies an increase in the impurity. Therefore, it seems reasonable to attribute the photoinduced modulation of the reflected light to the change in geometrical structure rather than to the chirality of the azobenzene molecule. As can be seen in figure 11, the *cis*-configuration of AzoA was induced by irradiation with UV light, leading to a decrease in T_{ChI} of the

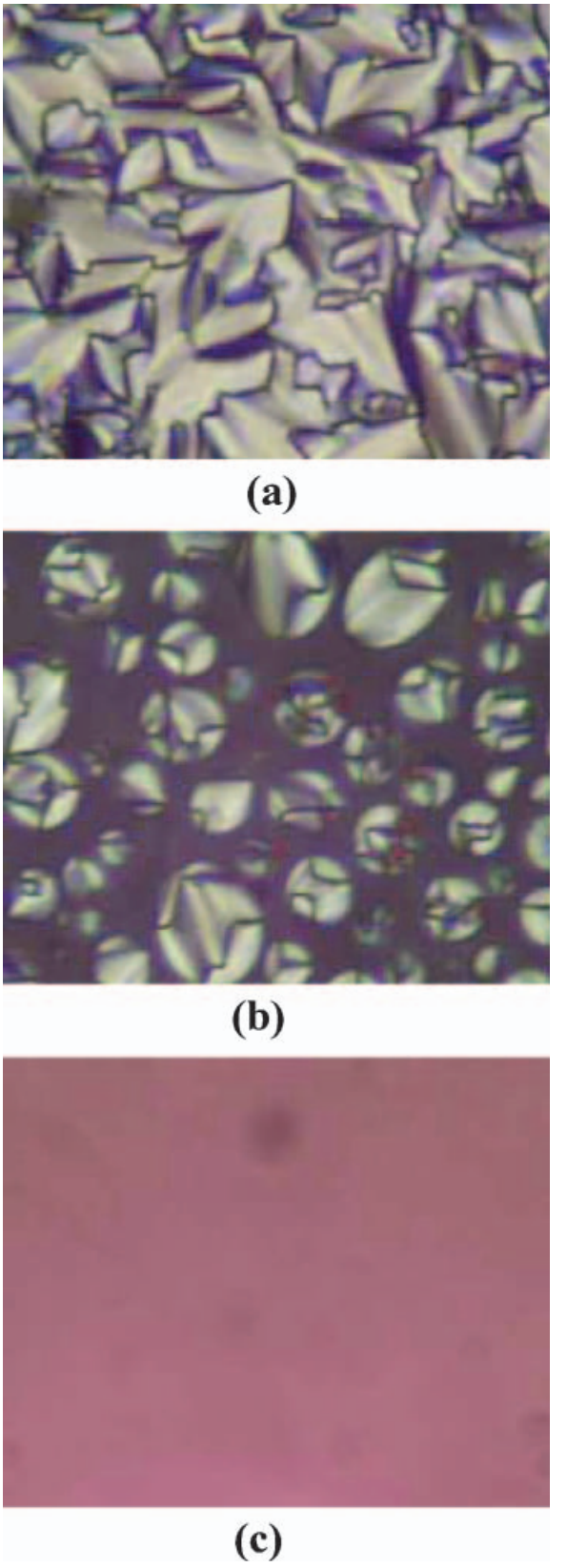

Figure 11. POM textures of cholesteric liquid crystal sample cell 12 with (*a*) 0, (*b*) 2 and (*c*) 5 min UV irradiation at 56°C.

Figure 12. Real image recording on sample cell 13 through a mask with 'Liu lab'.

cholesteric liquid crystal. Figure 11 (*c*) shows that the cholesteric LC orientation was completely destroyed by the photoinduced *cis*-AzoA molecules: after sufficient UV irradiation, an isotropic phase was generated and a dark POM picture was obtained.

Real image recording of the cholesteric LC cells fabricated in this investigation was also studied. Figure 12 shows an example of the photoinduced image through a Liu lab mask. Photoirradiated and non-irradiated areas appear as two different reflected colours, leading to the formation of the image.

4. Conclusions

Chiral compounds with various moieties were synthesized and identified using NMR, FTIR, and elemental analysis. Liquid crystal phases and optical rotation of the compounds were determined. To investigate the optical behaviour of cholesteric LC cells, host cells with various chiral dopants were fabricated. Thermal and UV irradiation effects on the cholesteric LC cells were investigated. Chirality and molecular interaction were found to be factors which affect the twisting power and the reflected wavelength of the cholesteric cells. The addition of azo-dopants depressed the clearing point of the cholesteric cells. UV irradiation of the cholesteric LC cells around the clearing point caused a *trans-cis* isomerization of the azo-dopant and generated an isotropic phase leading to a clear appearance. The capability for real image recording of the cholesteric LC cells was confirmed using UV irradiation through a mask.

Acknowledgements

The authors would like to thank the National Science Council (NSC) of the Republic of China (Taiwan) for financial support of this research under Contract No. NSC 92-2216-E006-003.

References

[1] H. Coles. *Handbook of Liquid Crystals*, Vol. 2A, D. Demus, J. Goodby, G.W. Gray, H.-W. Spiess, V. Vill (Eds), p. 365, VCH, Weinheim (1998).
[2] Y.K. Yarovoy, M.M. Labes. *Mol. Cryst. liq. Cryst.*, **270**, 101 (1995).
[3] A.Y. Bobrovsky, N.I. Boiko, V.P. Shibaev. *Liq. Cryst.*, **25**, 679 (1998).
[4] C. Ruslim, K. Ichimura. *J. phys. Chem. B*, **104**, 6529 (2000).
[5] M. Brehmer, J. Lub, P. van de Witte. *Adv. Mater.*, **17**, 1438 (1998).
[6] T. Ikeda, S. Horiuchi, D.B. Karanjit, S. Kurihara, S. Tazuke. *Macromolecules*, **23**, 36 (1990).
[7] T. Sasaki, T. Ikeda, K. Ichimura. *Macromolecules*, **25**, 3807 (1992).
[8] T. Ikeda, O. Tsutsumi. *Science*, **268**, 1873 (1995).
[9] A. Shisido, O. Tsutsumi, A. Kanazawa, T. Shiono, T. Ikeda, N. Tamai. *J. phys. Chem. B*, **101**, 2806 (1997).
[10] S. Kurihara, A. Sakamoto, T. Nonaka. *Macromolecules*, **31**, 4648 (1998).
[11] O. Tsutsumi, T. Shiono, T. Ikeda, G. Galli. *J. Phys. Chem. B*, **101**, 1332 (1997).
[12] O. Tsutsumi, A. Kanazawa, T. Shiono, T. Ikeda, L.-S. Park. *Phys. Chem. chem. Phys.*, **1**, 4219 (1999).
[13] A. Shishido, O. Tsutsumi, A. Kanazawa, T. Shiono, T. Ikeda, N. Tamai. *J. Am. chem. Soc.*, **119**, 7791 (1997).
[14] H.-K. Lee, A. Kanazawa, T. Shiono, T. Ikeda, T. Fujisawa, M. Aizawa, B. Lee. *J. appl. Phys.*, **86**, 5927 (1999).
[15] E. Sackmann. *J. Am. chem. Soc.*, **93**, 7088 (1971).
[16] H.-K. Lee, K. Doi, H. Harada, O. Tsutsumi, A. Kanazawa, T. Shiona, T. Ikeda. *J. phys. Chem.*, **104**, 7023 (2000).
[17] S. Kurihara, S. Nomiyama, T. Nonaka. *Chem. Mater.*, **12**, 9 (2000).
[18] S. Kurihara, S. Nomiyama, T. Nonaka. *Chem. Mater.*, **13**, 1992 (2001).
[19] C. Ruslim, K. Ichimura. *Adv. Mater.*, **13**, 37 (2001).
[20] C. Ruslim, K. Ichimura. *Adv. Mater.*, **13**, 641 (2001).
[21] G. Rodekirch, J. Rübner, V. Zschuppe, D. Wolff, J. Springer. *Makromol. Chem.*, **194**, 1125 (1993).
[22] L.K.M. Chan, G.W. Gray, D. Lacey, R.M. Scrowston, I.G. Shenouda, K.J. Toyne. *Mol. Cryst. liq. Cryst.*, **172**, 125 (1989).
[23] M. Rosario de la Fuente, M.A. Perez-Jubindo. *Chem. Mater.*, **13**, 2056 (2001).
[24] J.H. Liu, P.C. Yang. *J. appl. polym. Sci.*, **91**, 3693 (2004).
[25] J.H. Liu, H.Y. Wang. *J. appl. polym. Sci.*, **91**, 789 (2004).
[26] P. Witte, M. Brehmer, J. Lub. *J. mater. Chem.*, **9**, 2087 (1999).
[27] C. Ruslim, K. Ichimura. *J. Phys. Chem. B*, **104**, 6529 (2000).
[28] S. Kurihara, T. Yoshioka, T. Ogata, A. Zahangir, T. Nonaka. *Liq. Cryt.*, **30**, 1219 (2003).
[29] S. Kurihara, S. Nomiyama, T. Nonaka. *Chem. Mater.*, **13**, 1992 (2001).
[30] R.A. Delden. *Controlling Molecular Chirality and Motion*,, Baarn, Holland; Electronic Version: ISBN 90-367-1609-3, Chap. 3 (2002).
[31] H.-K. Lee, A. Kanazawa, T. Shiono, T. Ikeda, T. Fujisawa, M. Aizawa, B. Lee. *Chem. Mater.*, **10**, 1402 (1998).